Published in final edited form as:
Aging Cell. 2011 December ; 10(6): 996–1010. doi:10.1111/j.1474-9726.2011.00740.x.

Ablation of ghrelin receptor reduces adiposity and improves insulin sensitivity during aging by regulating fat metabolism in white and brown adipose tissues

Ligen Lin[1], **Pradip K. Saha**[2], **Xiaojun Ma**[1], **Iyabo O. Henshaw**[1], **Longjiang Shao**[3], **Benny H. J. Chang**[2], **Eric D. Buras**[2], **Qiang Tong**[1,2,3], **Lawrence Chan**[2,4], **Owen P. McGuinness**[5], and **Yuxiang Sun**[1,3,4,*]

[1]USDA/ARS Children's Nutrition Research Center, Department of Pediatrics, Baylor College of Medicine, Houston, TX, 77030

[2]Department of Medicine, Baylor College of Medicine, Houston, TX, 77030

[3]Huffington Center on Aging, Baylor College of Medicine, Houston, TX, 77030

[4]Department of Molecular and Cellular Biology, Baylor College of Medicine, Houston, TX, 77030

[5]Department of Molecular Physiology and Biophysics, Vanderbilt University School of Medicines, Nashville, TN, 37232

Summary

Aging is associated with increased adiposity in white adipose tissues and impaired thermogenesis in brown adipose tissues; both contribute to increased incidences of obesity and type 2 diabetes. Ghrelin is the only known circulating orexigenic hormone that promotes adiposity. In this paper, we show that ablation of the ghrelin receptor (growth hormone secretagogue receptor, GHS-R) improves insulin sensitivity during aging. Compared to wild-type (WT) mice, old *Ghsr*$^{-/-}$ mice have reduced fat and preserve a healthier lipid profile. Old *Ghsr*$^{-/-}$ mice also exhibit elevated energy expenditure and resting metabolic rate, yet have similar food intake and locomotor activity. While GHS-R expression in white and brown adipose tissues was below detection in the young mice, GHS-R expression was readily detectable in visceral white fat and interscapular brown fat of the old mice. Gene expression profiles reveal that *Ghsr* ablation reduced glucose/lipid uptake and lipogenesis in white adipose tissues, but increased thermogenic capacity in brown adipose tissues. *Ghsr* ablation prevents age-associated decline of thermogenic gene expression of uncoupling protein 1 (UCP1). Cell culture studies in brown adipocytes further demonstrate that ghrelin suppresses the expression of adipogenic and thermogenic genes, while GHS-R antagonist abolishes ghrelin's effects and increases UCP1 expression. Hence, GHS-R plays an important role in thermogenic impairment during aging. *Ghsr* ablation improves aging-associated obesity and insulin resistance by reducing adiposity and increasing thermogenesis. GHS-R antagonists may be a new means of combating obesity by shifting the energy balance from obesogenesis to thermogenesis.

Keywords

Ghrelin; GHS-R; obesity; insulin resistance; aging; thermogenesis

[*]**Correspondence to:** Yuxiang Sun, Children's Nutrition Research Center, Department of Pediatrics, Baylor College of Medicine, 1100 Bates St. Room 5024. Houston, TX 77030. Tel.: 713-798-7167; Fax: 713-798-9396; yuxiangs@bcm.edu.

Supporting information

Additional supporting information may be found in the online version of this article:

Introduction

Obesity often leads to insulin resistance, which can further lead to pancreatic β-cell failure and type 2 diabetes (Kahn *et al.* 2006). Type 2 diabetes is a serious threat for the elderly population; in the United States almost 1 in 5 elderly over age 65 has diabetes, mostly type 2 diabetes. The identification and characterization of the genes involved in the pathophysiology of obesity and insulin resistance have become a pressing challenge.

There are two types of adipose tissues: energy-storing white adipose tissue (WAT) and energy-burning brown adipose tissue (BAT). WAT stores energy in the form of triglycerides and supplies energy to the body as ATP through lipolysis/β oxidation. Visceral adiposity of WAT is a prominent risk factor for insulin resistance and type 2 diabetes, which is significantly elevated in obese individuals and elderly (Gabriely *et al.* 2002; Ahima 2009; Amati *et al.* 2009). In contrast to WAT, BAT is a key organ of non-shivering thermogenesis, playing an important role in energy expenditure. While WAT is made of big adipocytes, BAT consists of small adipocytes containing a reduced amount of triglyceride in multi-lobular lipid droplets, and has a high density of mitochondria (Cannon & Nedergaard 2004). UCP1 is a key regulator of thermogenesis in BAT; it allows protons to enter the mitochondrial matrix and enables mitochondria to dissipate heat (Inokuma *et al.* 2005; Feldmann *et al.* 2009). It is known that BAT is present in rodents and human neonates. BAT positively correlates with energy expenditure, and negatively correlates with fat mass. BAT is responsible for more than half of the total oxygen consumption in small animals (Cannon & Nedergaard 2004). It is only recently recognized that BAT is also present in adult humans, and that dysregulation of adaptive thermogenesis in BAT reduces energy expenditure and promotes obesity (van Marken Lichtenbelt *et al.* 2009; Nedergaard & Cannon 2010). Aging is associated with severely diminished thermogenesis (Lecoultre & Ravussin 2010; Mattson 2010; Pfannenberg *et al.* 2010). It was recently reported that in aged men, BAT activity decreased 75% and BAT mass decreased 95% when compared with younger men (Pfannenberg*et al.* 2010). BAT plays a critical role in fat metabolism and thermogenesis during aging, but the underlying molecular mechanisms of age-associated thermogenesis are totally unknown.

Ghrelin, a 28-amino acid acylated peptide, is the only circulating orexigenic hormone known to increase growth hormone (GH) release, and stimulate appetite and promote obesity (Tschop *et al.* 2000; Cowley *et al.* 2003; Shimbara *et al.* 2004; Sun *et al.* 2004; Kojima & Kangawa 2005). We reported that ghrelin deletion increases glucose-induced insulin secretion, and improves glycemic control in leptin-deficient *ob/ob* mice by reducing uncoupling protein 2 (UCP2) in pancreatic islets (Sun *et al.* 2006). This helped to establish ghrelin's novel role in glucose homeostasis and diabetes. We and others have also shown that ghrelin's effects on GH release and appetite are mediated through the activation of GHS-R (Sun *et al.* 2004; Andrews *et al.* 2008; Davies *et al.* 2009). Ghrelin is ubiquitously expressed, and the highest levels are detected in the stomach and intestine; in contrast, the expression of GHS-R is much more restricted (Gnanapavan *et al.* 2002). Using $Ghsr^{-/-}$ mice as control, we showed that in young mice, GHS-R1a (distinct from non-functional receptor GHS-R1b) mRNA is highly expressed in the pituitary and brain, and lower levels are detectable in organs such as pancreas, heart, thymus, lung, adrenal, small intestine, spleen, and kidney. However, GHS-R1a is not expressed in liver, skeletal muscle, white or brown adipose tissues of young mice (Sun *et al.* 2007b). We have shown previously that GHS-R knockout mice ($Ghsr^{-/-}$) have modestly reduced body weight and insulin-like growth factor 1 (IGF-1), but have a normal appetite (Sun *et al.* 2004). Furthermore, glucose and insulin levels are reduced in $Ghsr^{-/-}$ mice upon calorie restriction challenge (Sun *et al.*

2007a). These studies together suggest that the ghrelin signaling pathway may play an important role in energy- and glucose-homeostasis.

In the present study, we used *Ghsr*$^{-/-}$ mice to further investigate the role of GHS-R in obesity and insulin sensitivity during aging. We monitored wild-type (WT) and *Ghsr*$^{-/-}$ mice during natural aging with regular chow feeding. As the old WT mice become obese and insulin-resistant, old *Ghsr*$^{-/-}$ mice maintain a youthful metabolic state: lean, insulin-sensitive and having a higher resting metabolic rate. Surprisingly, we have detected GHS-R1a mRNA expression in epididymal WAT and interscapular BAT of old WT mice. We showed that GHS-R ablation prevents age-associated decline of thermogenic gene expression. Ablation of GHS-R reduces adiposity in energy-storing WAT, and increases thermogenesis in energy-burning BAT. Our data showed for the first time that GHS-R has opposite effects on WAT and BAT during aging, providing new insight into the pathophysiology of age-associated obesity and insulin resistance.

Results

Old *Ghsr*$^{-/-}$ mice display reduced adiposity and improved lipid profile

Initial observations of the young *Ghsr*$^{-/-}$ mice indicated a slightly lower body weight (Sun *et al.* 2004; Sun *et al.* 2008). We continued to monitor the body weights of the mice as they aged. The *Ghsr*$^{-/-}$ mice showed a consistent 10-15% reduction in body weight from 4- to 20-months old when compared with their WT littermates, and the body weight difference between the WT and null mice was even more pronounced between 22- to 26-months of age (Fig. 1A). We used PIXImus densitometer to quantify the whole-body composition. Old *Ghsr*$^{-/-}$ mice (18-22 months) had a 35% reduction in fat mass and a 10% increase of lean mass when compared with their WT littermates (Fig. 1B). Anatomic magnetic resonance imaging (MRI) analyses showed that old *Ghsr*$^{-/-}$ mice have dramatically reduced intra-abdominal and subcutaneous fat (Fig. 1C). The dissection of epididymal fat from old mice also supported the observation (Fig. S1.A). Thus, old *Ghsr*$^{-/-}$ mice have reduced body weight, which was primarily due to their reduced adiposity.

Serum levels of adipose-secreting hormones often correlate with the amount of lipid stored in WAT. While there was no difference in adiponectin and resistin (Fig. S1.B), fasting serum leptin levels were significantly lower in *Ghsr*$^{-/-}$ mice (Fig. 1D), indicative of reduced fat mass. Serum free fatty acid (FFA), triglycerides, cholesterol, and low-density lipoprotein (LDL) are positively correlated with obesity, which consequently causes insulin resistance, type 2 diabetes and cardiovascular disease (Kahn *et al.* 2006). To elucidate whether the old *Ghsr*$^{-/-}$ mice maintain a healthier lipid profile, the fasting serum lipid profiles of old WT and *Ghsr*$^{-/-}$ mice were analyzed. The fasting cholesterol, triglycerides, HDL, LDL and VLDL in *Ghsr*$^{-/-}$ mice were reduced when compared with WT controls (Fig. 1E). The FFA levels were elevated after 18-hour fasting in both WT and *Ghsr*$^{-/-}$ mice when compared with those of 4-hour fasted mice, and the fasted FFA of *Ghsr*$^{-/-}$ mice was significantly lower than that of WT mice (Fig. 1F). Together, these results show that deletion of GHS-R improves lipid profiles.

Old *Ghsr*$^{-/-}$ mice are protected against age-associated insulin resistance

It is well established that excess fat mass and high circulating FFA and triglycerides induce insulin resistance (Kahn *et al.* 2006). Reduced fat mass and improved lipid profile in *Ghsr*$^{-/-}$ mice led us to hypothesize that ablation of GHS-R might improve insulin sensitivity. Insulin tolerance tests (ITT) and glucose tolerance tests (GTT) were performed on young (2-4 months) and old (18-26 months) WT and *Ghsr*$^{-/-}$ mice. Young WT and *Ghsr*$^{-/-}$ mice were both sensitive to insulin, and the difference between WT and *Ghsr*$^{-/-}$

was not pronounced in ITT at 2-, 3- or 4-months of age (4-month data is shown as "young" in Fig. 2A). As the mice aged, ITT showed WT mice became severely insulin resistant. Remarkably, old *Ghsr*$^{-/-}$ mice were significantly more responsive to an insulin challenge when compared to WT mice at 18-, 20-, 24-, and 26-months of age, and maintained a response curve similar to that of insulin-sensitive young mice (20-month data is shown "as old" in Fig. 2A). During GTT, there was no difference in glucose clearance following a glucose load in young WT and *Ghsr*$^{-/-}$ mice, but remarkably, the insulin levels of the null mice were significantly lower, indicative of increased insulin sensitivity (Fig. 2B top panel). In old mice, *Ghsr*$^{-/-}$ mice showed faster glucose clearance and reduced insulin secretion during a GTT when compared with WT mice (Fig. 2B bottom panel, Fig. S2.A), again supporting a conclusion of improved insulin sensitivity. Together, these functional tests suggest that *Ghsr*$^{-/-}$ mice have improved peripheral insulin sensitivity during aging.

ITT and GTT are often considered stressful for the mice. To further define the insulin-sensitive phenotype, we performed "state-of-the-art" glucose and insulin clamps on conscious animals. In hyperinsulinemic-euglycemic clamps of young *Ghsr*$^{-/-}$ mice, while the basal endogenous glucose production was unaffected (Fig. 2C), the glucose infusion rate (GIR) was increased, which indicates increased glucose uptake in peripheral tissues. Using isotope tracer (^{14}C), we showed that glucose uptake was increased in muscle (Fig. 2C), but not in liver or fat. Surprisingly, however, in old animals no difference was detected in hyperinsulinemic-euglycemic clamps (Fig. S2.B). To further elucidate whether old *Ghsr*$^{-/-}$ mice are insulin-sensitive, hyperglycemic and hypoglycemic clamps were carried out to test the mice under extreme glycemic conditions. Hyperglycemic clamp study showed that old *Ghsr*$^{-/-}$ mice produced a markedly reduced insulin response compared to that of WT mice, indicative of requiring less insulin to maintain hyperglycemia (Fig. 2D). The hypoglycemic clamp study showed that old *Ghsr*$^{-/-}$ mice required higher glucose infusion to maintain hypoglycemia than WT mice (Fig. 2E). Results from these clamp experiments are consistent with the conclusion that *Ghsr*$^{-/-}$ mice are more sensitive to insulin under extreme glycemic conditions, and this phenotype becomes more pronounced during aging.

Old *Ghsr*$^{-/-}$ mice have increased energy expenditure

Energy balance is determined by energy intake and energy expenditure. Lean phenotype can result from reduced food intake and/or increased energy expenditure (increased activity and/or elevated thermogenesis). We employed indirect calorimetry to characterize the metabolic profiles of 22-month old WT and *Ghsr*$^{-/-}$ mice in order to decipher the cause(s) of the lean and insulin-sensitive phenotype of the old *Ghsr*$^{-/-}$ mice. The daily food intake of WT and *Ghsr*$^{-/-}$ mice was comparable during indirect calorimetry (Fig. 3A), indicating that energy intake is not a determining factor of the lean phenotype. We then speculated that *Ghsr*$^{-/-}$ may have increased energy expenditure due to elevated activity and/or enhanced thermogenesis. However, the locomotor activity of *Ghsr*$^{-/-}$ mice didn't differ from that of WT control mice, (Fig. 3B), indicating that activity also is not a determining factor of the lean phenotype. Remarkably however, the oxygen consumption (VO_2) and carbon dioxide production of *Ghsr*$^{-/-}$ mice were significantly elevated (Fig. 3C corrected by lean mass; S3.A-B corrected by body weight). Old *Ghsr*$^{-/-}$ mice show significantly higher energy expenditure (Kcal/h/Kg body weight) when compared with WT mice (Fig. S3.C). Recent literature has questioned whether body weight is the right correcting factor for energy expenditure when comparing animals which have different body composition (Butler & Kozak 2010). Thus, we also calculated energy expenditure corrected by lean mass (Kcal/h/Kg lean), and found that old *Ghsr*$^{-/-}$ mice consistently showed an elevated energy expenditure (Fig. 3D). Furthermore, we analyzed resting metabolic rate (RMR) to evaluate the metabolic state of the mice, and our data demonstrated that old *Ghsr*$^{-/-}$ mice have an increased RMR (Fig. 3E). In addition, respiratory quotient (RQ) was increased during both

light and dark cycles (Fig. 3F), indicating that the *Ghsr*$^{-/-}$ mice favor carbohydrates as a fuel substrate. Metabolic flexibility, defined as the capacity of the organism to adapt fuel oxidation to fuel availability, is used as an indicator of insulin-sensitivity; relative cumulative frequency (RCF) is a method for evaluating metabolic flexibility (Riachi *et al.* 2004). Old *Ghsr*$^{-/-}$ mice had broader RQ distributions when compared with their WT counterparts, indicating a higher metabolic flexibility (Fig. 3G). The metabolic profile data showed that ablation of GHS-R resulted in increased energy expenditure and RMR, and improved metabolic flexibility. No difference was detected in any of the aforementioned metabolic parameters in young (3-month old) WT and *Ghsr*$^{-/-}$ mice (data not shown). Collectively, the data suggest that the insulin-sensitive lean phenotype of old *Ghsr*$^{-/-}$ mice is likely due to increased energy expenditure, rather than changes caused by energy intake or activity.

Ablation of GHS-R reduces size of adipocytes through reduction of fat synthesis in white adipose tissues

Epididymal fat in rodents is commonly used as representative of a visceral fat depot because it has many characteristics of visceral fat in humans (Miegueu *et al.* 2011). Our previous studies showed that GHS-R1a is not expressed in epididymal fat of young mice (Sun *et al.* 2007b). However, intriguingly, our real-time RT-PCR analysis of old mice between 18- to 26-months of age showed consistently low levels of GHS-R1a mRNA expression were detectable in epididymal fat, but not in subcutaneous fat (Fig. 4A).

Aging is associated with increased adiposity. In order to determine whether the increased GHS-R expression in epididymal fat is a response to aging, but not adiposity *per se*, we compared GHS-R expression in epididymal fat of 13-month old WT mice which were fed either regular diet (RD) or high fat diet (HFD). Our data showed that these HFD-fed WT mice were significantly obese and insulin resistant (data not shown). Interestingly, GHS-R expression in epididymal fat was comparable between RD- and HFD-fed WT mice (Fig. S4.A). Similarly GHS-R expression was also not elevated in obese and insulin-resistant leptin-deficient *ob*/*ob* mice (Fig. S4.A). This data further supports our conclusion that the elevated GHS-R expression is more likely associated with aging, but not obesity. The age-dependent GHS-R expression in different types of fat depots suggests that GHS-R may have a direct effect in epididymal fat in regulating adiposity and insulin resistance during aging.

To further evaluate the adiposity of young and old *Ghsr*$^{-/-}$ mice, different fat depots of age-matched WT and *Ghsr*$^{-/-}$ mice were dissected and weighed. The weights of all fat depots increase with age (Fig. 4B). Consistent with the body composition and MRI imaging results, there were significant weight reductions in WAT fat depots in old *Ghsr*$^{-/-}$ mice. The visceral (e.g., epididymal) and subcutaneous (e.g., inguinal) fat of old *Ghsr*$^{-/-}$ mice were significantly lower than that of old WT mice, while the weights of these adipose depots in young mice were comparable between WT and *Ghsr*$^{-/-}$ mice (Fig. 4B).

Lower fat mass in old *Ghsr*$^{-/-}$ mice could be due to a decrease of adipocyte cell size or cell number. It is known that small adipocytes are more sensitive to insulin (Okuno *et al.* 1998; Roberts *et al.* 2009). Our histological analysis of epididymal fat showed that old *Ghsr*$^{-/-}$ mice have smaller adipocytes (Fig. 4C), which is in line with the insulin-sensitive phenotype of the *Ghsr*$^{-/-}$ mice. Quantitative analysis of the size of epididymal adipocytes indicated that *Ghsr*$^{-/-}$ mice had more small adipocytes and far fewer big adipocytes (Fig. 4D). The average adipocyte size of WT mice was 9316 μm^2, and average adipocyte size of *Ghsr*$^{-/-}$ mice was 5113 μm^2. The adipocyte cell numbers were also evaluated, using triglyceride content (Okuno *et al.* 1998); there was no difference in cell numbers between WT and *Ghsr*$^{-/-}$ mice (Fig. 4E). Therefore, the marked decrease in fat mass of *Ghsr*$^{-/-}$ mice was due to a reduction in adipocyte cell size, but not cell number.

Old *Ghsr*$^{-/-}$ mice have lower fat mass. Fat mass is determined by fat synthesis (adipogenesis/lipogenesis) and fat mobilization (lipolysis/β oxidation) (Kersten 2001). To determine the underlying molecular mechanisms, epididymal fat was collected from 20- to-24-month old WT and *Ghsr*$^{-/-}$ mice, and the mRNA expression of adipogenic, lipogenic, lipolytic and lipid recycling genes was assessed using real-time RT-PCR (Table 1). PPARγ2 and C/EBPα are important regulators for adipogenesis. PPARγ2 was significantly down-regulated in the *Ghsr*$^{-/-}$ mice but C/EBPα was unchanged, suggesting that adipogenesis may not be a key mechanism. The expression of glucose uptake (GLUT4) and lipid uptake (LPL, CD36) genes were markedly reduced, suggesting reduced substrate uptake. The expression of lipogenesis markers (aP2, FAS, and lipin1) was also significantly reduced in *Ghsr*$^{-/-}$ mice, suggesting reduced lipogenesis. Gene expression profiles above collectively support that *Ghsr* ablation inhibits lipid synthesis. Perilipin is a lipid droplet-protective protein, and down-regulation of perilipin is associated with increased lipolysis; while hormone-sensitive lipase (HSL) is a key lipolytic enzyme, and down-regulation of HSL is associated with decreased lipolysis (Saha *et al.* 2004; Kovsan *et al.* 2009). We observed decreased mRNA expression of both perilipin and HSL in the epididymal fat of the old null mice. Thus, lipolysis may not play a major role in GHS-R mediated lipid metabolic regulation in WAT, and the reduced expression of perilipin and HSL may simply reflect the reduced lipid droplets in the null mice. In addition, a lipid recycling gene PEPCK was down-regulated, the fat utilization gene (UCP2) was unchanged, and cholesterol exporter gene (ABCG1) was modestly reduced. Since the fat mass is also reduced in subcutaneous fat, we also studied lipid metabolic gene expression in inguinal fat. Down-regulation of the genes involved in adipogenesis, glucose/lipid uptake, lipogenesis and lipid utilization was detected in inguinal fat (Supplemental Table), which is similar to the gene expression profile detected in epididymal fat. Collectively, the data suggest that the reduction of fat mass in old *Ghsr*$^{-/-}$ mice is mainly due to decreased glucose/lipid uptake and reduced lipogenesis in WAT.

Deletion of *Ghsr* increases lipid anabolic capacity and elevates thermogenic gene expression in brown adipose tissues

Increased energy expenditure in old *Ghsr*$^{-/-}$ mice is independent of their physical activity, which led us to hypothesize that GHS-R ablation may enhance thermogenesis. Our real time RT-PCR and semi-quantitative RT-PCR data showed that GHS-R1a mRNA was detected in BAT of old, but not in young mice (Fig. 5A). In order to decipher whether the increased GHS-R expression in BAT is a response to aging, but not to adiposity *per se*, we compared GHS-R expression in BAT of 13-month old WT mice fed either RD or HFD. While the expression of UCP1 in BAT was robustly increased in HFD-fed mice as expected, no increase was detected with GHS-R expression (Fig. S4.B). This result supports that GHS-R expression in BAT of old mice is likely associated with aging, but not obesity, suggesting that GHS-R may have direct effect on BAT function as the animals age. BAT mass and/or activity are determinants of thermogenic capacity; aging is associated with reduced BAT mass and activity (Mattson 2010; Pfannenberg *et al.* 2010). As expected, the BAT percentage is significantly reduced in old mice regardless of genotype, but there was no difference in BAT mass between old WT and *Ghsr*$^{-/-}$ mice (Fig. 5B). The H&E staining of BAT sections of old *Ghsr*$^{-/-}$ mice showed a higher percentage of multilobular adipocytes and increased cellularity (dark blue nuclei), as shown in Fig. S5. PGC-1α is an upstream regulator of UCP1 (Inokuma *et al.* 2005). As shown in Table 2, PGC-1α expression was modestly increased in the old *Ghsr*$^{-/-}$ mice when compared to that of WT mice. As expected, UCP1 mRNA expression levels were decreased in BAT of old WT mice when compared to that of young WT mice (Fig. 5C). While there was no significant difference in UCP1 expression in BAT between young WT and *Ghsr*$^{-/-}$ mice, UCP1 expression in BAT of old *Ghsr*$^{-/-}$ mice was significantly higher than that of old WT mice, maintaining a level that is similar to young mice (Fig. 5C). We further demonstrated that the UCP1 protein

expression in BAT of old *Ghsr*$^{-/-}$ mice was significantly higher than that of old WT mice (Fig. 5D). The elevated expression of thermogenic genes indicates increased thermogenic capacity in BAT of the old *Ghsr*$^{-/-}$ mice. Consistently, the mitochondrial density characterized by ratio of mitochondrial DNA:nuclear DNA was increased in BAT of the old null mice (Fig. 5E); this supports our conclusion that the BAT of the old null mice have higher mitochondrial density. To further validate our results, we measured the rectal temperature (a good "read out" of core body temperature) of old (18-20 months) WT and *Ghsr*$^{-/-}$ mice. Indeed, the rectal temperature of old *Ghsr*$^{-/-}$ mice was significantly higher than that of WT mice, and the difference became more pronounced at an ambient temperature of 4°C, increasing from 0.67°C at 0 hour to 3.50°C after 4 hours of cold exposure (Fig. 5F).

An adequate supply of fatty acids is essential for BAT non-shivering thermogenesis (Festuccia*et al.* 2009). In agreement, increased expression of genes in regulating substrate uptake (GLUT4, LPL and CD36) and lipogenesis (aP2, Lipin1) was detected in BAT of *Ghsr*$^{-/-}$ mice (Table 2). The adipogenic markers PPARγ2 and C/EBPα were elevated, but only C/EBPα level reached statistical significance. The lipolytic gene expression showed that perilipin was increased, but HSL was unchanged. Together, these gene expression profiles suggest that old *Ghsr*$^{-/-}$ mice have increased glucose/lipid uptake and increased lipogenesis in BAT. The data collectively suggest that GHS-R regulates thermogenic function in BAT, and GHS-R ablation prevents the age-associated decline of thermogenesis.

Ghrelin, via GHS-R, directly regulates adipogenic and thermogenic genes in brown adipocyte HIB1B cells

To further address the direct effect of the ghrelin signaling pathway in BAT, we studied the expression of GHS-R1a in mouse brown adipose-derived HIB1B cells. GHS-R1a mRNA was expressed in both undifferentiated (day 0) and differentiated HIB1B cells (days 2-6) (Fig. 6A). To evaluate the role of ghrelin in thermogenic activation of HIB1B cells, saline or ghrelin (0.01 or 1 nM) was added to the cultures at day 0, day 2, day 4, and day 6. Interestingly, the adipogenic markers PPARγ2 and C/EBPα, and thermogenic regulators PGC-1α and UCP1, were significantly suppressed upon ghrelin treatment (Fig. 6B). To further elucidate the direct effect of GHS-R on thermogenic regulation in HIB1B cells, GHS-R antagonist, [D-Lys^3] -GHRP-6, was added to the cultures at day 0, day 2, day 4 and day 6. As expected, [D-Lys^3]-GHRP-6 increased UCP1 expression significantly (Fig. 6C), supporting that antagonism of GHS-R enhances thermogenic capacity. Interestingly, [D-Lys^3]-GHRP-6 also up-regulates PPARγ2, suggesting that GHS-R antagonist may also affect brown adipocyte differentiation (Fig. 6C). It is also important to note that [D-Lys^3]-GHRP-6 abolished ghrelin's inhibitory effects on PPARγ2, C/EBPα, PGC-1α, and UCP1 (Fig. 6C). The data together suggest that ghrelin, via GHS-R, directly inhibits differentiation and thermogenic activity of brown adipocytes. This is consistent with the gene expression profile we observed in BAT of *Ghsr*$^{-/-}$ mice (Table 2).

Discussion

Our study is the first report on chow-fed *Ghsr*$^{-/-}$ mice during normal aging up to 26-months of age. Old *Ghsr*$^{-/-}$ mice fed on regular chow have reduced fat mass, improved lipid profile (Fig. 1), and markedly improved insulin sensitivity (Fig. 2A and 2B), similar to high fat-fed young adult *Ghsr*$^{-/-}$ mice reported by others (Zigman *et al.* 2005; Longo *et al.* 2008). Interestingly, during hyperinsulinemic-euglycemic clamps, only young *Ghsr*$^{-/-}$ mice exhibit increased glucose infusion, but not old *Ghsr*$^{-/-}$ mice (Fig. 2C and Fig. S2.B). At the same time, old *Ghsr*$^{-/-}$ mice clearly showed improved insulin sensitivity during hyperglycemic and hypoglycemic clamps (Fig. 2D and 2E), suggesting that the insulin-sensitive phenotype of old *Ghsr*$^{-/-}$ mice is more pronounced under challenging conditions. We previously

reported that ghrelin ablation increases insulin secretion as a result of lowering UCP2 (Sun *et al.* 2006). Here, we demonstrated that ablation of GHS-R attenuates age-associated obesity and insulin resistance, maintaining a healthier metabolic profile. These data suggest that the ghrelin signaling pathway plays an important role in glucose homeostasis by regulating both insulin secretion and insulin actions.

With no difference in food consumption (Fig. 3A), the body weight and fat mass of old *Ghsr*$^{-/-}$ mice were lower compared to WT mice (Fig. 1A and 1B), suggesting old *Ghsr*$^{-/-}$ mice might have increased energy expenditure. Indeed, the old *Ghsr*$^{-/-}$ mice exhibited higher energy expenditure (Fig. 3D). Increased energy expenditure could result from increased physical (locomotor) activity, higher resting metabolic rate (RMR), and/or increased thermogenesis. Our results show that the locomotor activity is unchanged (Fig. 3B). RMR is an important parameter in determining energy balance, which accounts for ~60% of total energy expended (Tentolouris *et al.* 2006); and thyroid hormones are important regulators of RMR (Roti *et al.* 2000). *Ghsr*$^{-/-}$ mice have a higher RMR (Fig. 3E), but total serum T3 and T4 levels were no different between old WT and *Ghsr*$^{-/-}$ mice (Fig. S6). This suggests that the elevated RMR of old *Ghsr*$^{-/-}$ mice is not due to changes in circulating thyroid hormones, but we cannot preclude enhanced thyroid hormone activity at hypothalamus in the *Ghsr*$^{-/-}$ mice (Lopez *et al.* 2010). Thus, the increased energy expenditure observed in old *Ghsr*$^{-/-}$ mice is likely due to increased thermogenesis.

RQ is an indicator of fuel preference. Previously, it was reported that ghrelin increases RQ in rats and mice (Tschop *et al.* 2000; Theander-Carrillo *et al.* 2006), and *Ghsr*$^{-/-}$ mice showed reduced RQ under HFD feeding (Zigman *et al.* 2005). Interestingly, in the old *Ghsr*$^{-/-}$ mice fed normal chow, we detected higher RQ (Fig. 3F), which indicates that they favor carbohydrate as a fuel substrate. The elevated RQ may be due to reduced lipid supply in the lean old *Ghsr*$^{-/-}$ mice, thus forcing the mice to use more carbohydrate instead of fat. We detected increased GLUT4 in BAT, and increased glucose uptake in the muscle of the null mice (Fig. 2C). Increased glucose uptake in BAT and muscle of *Ghsr*$^{-/-}$ mice may contribute to the higher RQ. Old *Ghsr*$^{-/-}$ mice have greater RCF (Fig. 3G), which indicates the null mice have greater metabolic flexibility, consistent with the insulin-sensitive phenotype. Collectively, our data support that *Ghsr* ablation increases energy expenditure, RMR, and metabolic flexibility during aging, thereby maintaining a youthful, insulin-sensitive metabolic state.

During the preparation of this manuscript, another group reported that suppression of GHS-R using anti-sense RNA activates BAT and decreases fat storage in rats, and the effects were more pronounced under high fat feeding (Mano-Otagiri *et al.* 2010). Similar to our study, their GHS-R suppressed rats were lean and had increased energy expenditure. In contrast to our study, calorie intake and locomotor activity were increased in those rats. Our old *Ghsr*$^{-/-}$ mice exhibited a lean and insulin-sensitive phenotype with increased energy expenditure, but neither their food intake nor their activity levels were changed (Fig. 3A and 3B). Our data provide the first evidence that GHS-R regulates fat metabolism without affecting appetite or activity. Calorie restriction is the only proven intervention which prolongs lifespan. Low blood glucose, low triglycerides, and low insulin are the characteristic metabolic hallmarks of calorie-restricted subjects and centenarians (Barzilai *et al.* 1998; Barzilai & Gabriely 2001). Our *Ghsr*$^{-/-}$ mice have all these youthful health traits. GHS-R antagonists may offer great promise for novel interventions to mimic calorie restriction without diet or exercise.

Increasing evidence has shown that adipocyte cell size, but not adipocyte cell number, is correlated with insulin resistance (O'Connell *et al.* 2010). Larger adipocytes exhibit elevated lipolysis and secrete more FFA into the circulation, resulting in fatty acid toxicity in insulin-

responsive organs (Raz *et al.* 2005). Histological data revealed that decreased fat mass in old *Ghsr*$^{-/-}$ mice was mainly due to the reduction of cell size, rather than decreased cell number (Fig. 4C-E), which is consistent with the insulin-sensitive phenotype. We previously showed that *Ghsr*$^{-/-}$ mice have reduced circulating glucose levels under fasting condition (Sun *et al.* 2008). In the current study, the levels of circulating cholesterol, triglycerides, and fasting FFA levels were lower in the old *Ghsr*$^{-/-}$ mice (Fig. 1E and 1F). As shown in Table 1 of epididymal fat and the Supplemental Table of inguinal fat, the expression levels of glucose/lipid uptake genes (GLUT4, lipoprotein lipase and CD36) were dramatically down-regulated. Similarly, expression levels of lipogenic genes (aP2, FAS, Lipin 1) were also lower. These data suggest that reduced glucose/lipid uptake and lipogenesis could contribute to the reduced WAT mass of *Ghsr*$^{-/-}$ mice. Also as shown in Table 1, GHS-R ablation also appeared to decrease adiposity by promoting lipid export (ABCG) and/or inhibiting lipid recycling (PEPCK). Thus, GHS-R ablation may reduce fat mass of WAT by regulating lipid uptake, lipogenesis, lipid storage, lipid recycling, and/or lipid export.

BAT plays an important role in energy expenditure by regulating thermogenesis; BAT mass and activity show severe impairment during aging (Pfannenberg *et al.* 2010). It is intriguing that GHS-R expression was only detectable in BAT of old WT mice, but not young WT mice (Fig. 5A); this suggests that GHS-R may play a unique role in thermogenic regulation during aging. Our results showed that while the weight of BAT was significantly reduced in old mice as expected, there was no difference in weight of BAT between WT and *Ghsr*$^{-/-}$ mice at either young or old age (Fig. 5B). UCP1 expression decreases with age, and correlates with age-associated thermogenic impairment. Remarkably, BAT of old GHS-R mice maintained a level of UCP1 similar to that of young mice (Fig. 5C). The higher mRNA and protein expression levels of UCP1 and higher mitochondrial density detected in old *Ghsr*$^{-/-}$ mice suggest that GHS-R ablation improves thermogenic function and protects against aging-associated decline of thermogenesis (Fig. 5C-E). Indeed, we detected significantly higher core temperatures in the old *Ghsr*$^{-/-}$ mice (Fig. 5F). Body temperature is typically tightly regulated. The increased body temperature of old *Ghsr*$^{-/-}$ mice is significant, because it has been shown that increased body temperature of about 1°C could thermodynamically correspond to a 10% increase in metabolic rate (Cannon & Nedergaard 2010). Furthermore, old *Ghsr*$^{-/-}$ mice have significantly reduced subcutaneous fat; reduced subcutaneous fat can reduce insulating capacity and lead to increased heat loss. Thus, the difference we detected may be understated due to increased radiated heat loss; the amount of heat generated in GHS-R null mice is likely to be much higher than that reflected by core body temperature.

In direct contrast to WAT, all lipid metabolic genes in BAT were up-regulated (Table 2). Glucose and lipid uptake (GLUT4, LPL and CD36) and lipogenesis (aP2) genes were significantly increased in the BAT of *Ghsr*$^{-/-}$ mice, suggesting increased lipid uptake/synthesis. These results suggest that deletion of GHS-R may activate lipid synthesis machinery and increase lipid anabolic capacity in BAT, thus enhancing mitochondrial thermogenesis. Since elevated heat generation in BAT requires a huge amount of energy, lipid in BAT of the null mice may be quickly mobilized to generate heat. Thereby, even though lipid anabolic capacity is elevated in BAT of *Ghsr*$^{-/-}$ mice, no increased lipid accumulation could be detected (Fig. S5). Triglyceride and glucose are oxidizable substrates for thermogenesis. The elevated thermogenesis (heat production) in BAT of the null mice may subsequently diminish the lipid substrates in circulation, which may further promote fat mobilization in WAT, and then lead to reduced fat mass and improved insulin sensitivity.

Since our *Ghsr*$^{-/-}$mice are global knockout, the effects in adipose tissues we detected could be direct or indirect, central or peripheral. We detected down-regulation of the lipid metabolic genes in subcutaneous fat of old GHS-R null mice (Supplemental Table), but we

failed to detect GHS-R expression in subcutaneous fat of old WT mice (Fig. 4A). This suggests that the lipid metabolic effect of GHS-R in subcutaneous fat is likely an indirect effect. On another note, we detected more pronounced body weight difference as mice aged when GHS-R is expressed in adipose tissues (Fig. 1A); in the same time, we also detected modest body weight difference in young mice when GHS-R is hardly detectable in adipose tissues (Fig. 4A and 5A). The body weight difference in young mice may not be explained by GHS-R expression in adipose tissues. GHS-R is expressed at a high level in the brain (hypothalamus) starting from a young age, and hypothalamus is also known to play a role in thermogenesis and energy homeostasis. It is possible that the weight difference in the young mice reflects the central effect of GHS-R.

Our data in the old mice showed that low levels of GHS-R were detectable in epididymal WAT and interscapular BAT (Fig. 4A and Fig. 5A). The expression of GHS-R1a in white and brown adipose tissues is low, which invites the question of whether the expression is real and physiologically meaningful. We believe that a low-level of expression could still have significant impacts on biological functions, depending upon the binding partners and signaling cascades. To determine whether the expression of GHS-R is age-dependent but not obesity-dependent, we studied the expression of GHS-R in epididymal fat and BAT of diet-induced obese mice. While our data clearly showed an elevated diet-induced thermogenesis in the BAT of (insert it) obese mice, the GHS-R expression in WAT and BAT remained unchanged (Fig. S4). This further supports our conclusion that GHS-R expression is correlated with age but not obesity. Our result of GHS-R1a expression in visceral WAT of aging mice is consistent with reports in adipose tissues of old rats (Choi *et al.* 2003; Davies *et al.* 2009), and GHS-R is expressed at higher levels in rat epididymal fat than in subcutaneous fat (Davies *et al.* 2009). We have shown that circulating ghrelin levels and mRNA expression of brain and pituitary GHS-R increase with age (Sun *et al.* 2007b), which may suggest that there is an increase in “ghrelin resistance” during aging. GHS-R may be “turned on” in those fat depots during aging, and play a causative role in age-associated obesity and insulin resistance. In line with our observation, chronic *i.v.* infusion of ghrelin into rats has been shown to induce a depot-specific increase in WAT mass, and ghrelin’s effect on adiposity has been shown to be attenuated in $Ghsr^{-/-}$ mice (Choi *et al.* 2003; Davies *et al.* 2009). An animal model of GHS-R inducible systems turning GHS-R on or off during aging may provide further direct evidence as to whether the dysregulation of GHS-R plays a key role in fat metabolism during aging. Increased obesity and insulin resistance in mice during aging may be explained by the activation of the GHS-R pathway in the white and/or brown fat depots.

To determine whether GHS-R has direct effects on lipid metabolism in white and brown adipocytes, we studied expression of GHS-R1a in white adipose-derived cell line 3T3-L1. We were not able to detect GHS-R1a expression in either undifferentiated or differentiated 3T3-L1 cells (data not shown). Interestingly, GHS-R mRNA expression was readily detectable in both undifferentiated and differentiated brown adipose HIB1B cells (Fig. 6A). Ghrelin strongly suppresses the expression of differentiation regulator PPARγ and thermogenic regulator UCP1 in HIB1B cells (Fig. 6B). In contrast, GHS-R antagonist [D-Lys^3]-GHRP-6 has opposite effects on PPARγ and UCP1, and abolishes ghrelin’s inhibitory effects (Fig. 6C). This data is in line with our gene expression data of BAT in Table 2, and further supports our *in vivo* observation that GHS-R antagonism increases differentiation and thermogenic capacity of brown adipocytes. The data more importantly suggests that ghrelin, via GHS-R, may directly regulate lipid metabolism and thermogenesis in BAT.

Our data provide the first evidence that GHS-R is an important regulator of lipid metabolism during normal aging, and *Ghsr* ablation increases energy expenditure through up-regulation of thermogenic function. Increased GHS-R expression in fat during aging may promote

impairment of thermogenesis, and contribute to aging-associated obesity and insulin resistance. *Ghsr* ablation prevents age-associated decline of thermogenic gene expression in BAT, and ghrelin/GHS-R has direct thermogenic effects in brown adipocytes, suggesting that GHS-R may directly regulate thermogenesis in BAT. Our data showed that GHS-R ablation has effects on both energy-storing WAT and energy-burning BAT: reducing adiposity in WAT to reduce energy substrates, and activating heat production in BAT to increase energy expenditure (Fig. 7). This unique property of GHS-R suggests that GHS-R antagonists may serve as new anti-obesity and anti-insulin resistance drugs shifting metabolic states from obesogenic to a thermogenic.

Experimental procedures

Animals

Ghsr$^{-/-}$ mice in C57BL/6J background were generated and genotyped as described previously (Sun *et al.* 2004). All mice used in the experiments are congenic (backcrossed 13 generations to C57BL/6J background) male mice. Wild-type (WT) and homozygous knockout mice (*Ghsr*$^{-/-}$) were housed and bred in a pathogen-free facility at Baylor College of Medicine. Animals were housed under controlled temperature and lighting (75±1 °F; 12h light-dark cycle) with free access to food and water. All diets from Harlan-Teklad, and the diet compositions are as follows: control chow (2920X, 16% of calories from fat, 60% from carbohydrates, 24% from protein); or a high-fat diet (“Western diet”, TD 88137, 42% of calories from fat, 43% from carbohydrates,15% from protein). All experiments were approved by the Animal Care Research Committee of the Baylor College of Medicine. To determine data-relevant age cohorts, we tested young mice at 2-, 3-, and 4-months of age, and old mice at 18-, 20-, 24-, and 26-months of age. We found that the data results were similar from 2- to 4-months of age, and 18- to 26 months of age, respectively. The figures presented in the papers are representative data.

Metabolic characterizations

Serum cholesterol was determined with a Cholesterol/Cholesteryl Ester Quantitation Kit (BioVision). Plasma triglyceride levels were analyzed by a Serum Triglyceride Determination Kit (Sigma). LDL, HDL and LVDL were determined by homogeneous enzymatic colorimetric methods. Plasma leptin, adiponectin, and resistin levels were measured by Linco Research, Inc., using a mouse leptin RIA kit. Plasma FFA was measured with an enzymatic colorimetric NEFA C Test Kit by Wako Chemicals (Richmond, VA). .

Mice body composition were analyzed with a Lunar PIXImus densitometer (Lunar Corp., Madison, WI), equipped for dual energy X-ray absorptiometry (DEXA). MRI analysis of body composition was also carried out using an EchoMRI Whole Body Composition Analyzer (Echo Medical Systems). Anatomical MRI experiments were performed utilizing a Bruker Pharmascan 7.0-T spectrometer, 16cm-bore, horizontal imaging system (Bruker Biospin, Billerica, MA) with a 38-mm volume resonator. All imaging was respiratory-gated. During the imaging, the animal body temperature was maintained at 37.0°C using an animal heating system (SA Instruments, Stony Brook, NY). For each mouse, images were acquired for 20 axial slices and 20 coronal slices, with 1.0-mm thickness. To get the best contrast for fat tissue, a T1-weighted spin-echo sequence was used for imaging with the following parameters: repetition time = 500ms, echo time = 10.7ms, field of view = 50.0mm × 45.0mm (coronal slices) and 45.0 × 45.0mm (axial slices), matrix size of 256 × 256; two signal averages were acquired.

Metabolic parameters were obtained using an Oxymax open-circuit indirect calorimetry system (Columbus Instruments, Columbus, OH). Briefly, oxygen consumption (VO_2) and

carbon dioxide production (VCO_2) by each animal was measured for a 48h period. Respiratory quotient (RQ) ratio of VCO_2/VO_2 was then calculated. Energy expenditure (or heat) was calculated as the product of the calorific value of oxygen (3.815 +1.232 * RQ) and the volume of O_2 consumed. Resting metabolic rate (RMR) was determined by selecting the three lowest points of the energy expenditure curve during each light cycle; this corresponds to resting periods, as previously described (Nuotio-Antar *et al.* 2007).

The percent relative cumulative frequency (PRCF) is a quantitative approach, which is used to detect small differences in energy metabolism (Riachi *et al.* 2004). The approach involves sorting data in ascending order, calculating their cumulative frequency, and then expressing the frequencies in the form of percentile curves. Statistical comparisons of PRCF curves are based on the 50th percentile values and curve slopes (H values). The 50th percentile value represents the mean RQ. The slope of a PRCF graph of RQ results is inversely related to the degree of metabolic flexibility between the oxidation of fatty acids and carbohydrates.

Histological analysis

Tissues (WAT and BAT) were fixed overnight in 10% formalin at room temperature, dehydrated and then embedded in paraffin. Tissue blocks were then sectioned at 5 μm for H&E staining. The H&E staining were carried out following the standard protocols (Stevens 1996).

Insulin tolerance test and glucose tolerance test

The insulin tolerance tests (ITT) were carried out on the young and old male mice. After being fasted for 6h, mice tail blood glucose concentration was measured using the commercially available OneTouch Ultra blood glucose meter and test strips (LifeScan). Mice then received an i.p injection of human insulin (Eli Lilly) at a dose of 0.75-1.0 U/kg of body weight. Tail blood glucose concentration was measured at 0, 30, 60, 90, and 120min after injections. The glucose tolerance tests (GTT) were carried after the mice were fasted for 18h. The mice then received an i.p. injection of glucose solution (Sigma-Aldrich) at a dose of 2.0-2.5 g/kg body weight. The mice tail blood glucose was measured at 0, 15, 30, 60 and 120min after injections.

Hyperinsulinemic-euglycemic, hyperglycemic and hypoglycemic clamp studies

For hyperinsulinemic-euglycemic clamp of young mice (2-months): jugular vein was catheterized, and the clamp experiment was performed as previously described (Saha *et al.* 2004). Briefly, after being fasted overnight, mice were administered a primed infusion (10 μCi), and then a constant rate intravenous infusion (0.1 μCi/min), of high pressure liquid which was chromatography-purified [3-^{3}H]glucose (PerkinElmer Life Sciences), using a syringe infusion pump (KD Scientific). For determination of basal glucose production, blood samples were collected from the tail vein after 50, 55, and 60min from the start of labeled glucose infusion. After 60 min, mice were primed with regular insulin (bolus 16 milliunits/kg body weight), followed by a 2-hr insulin infusion (4 milliunits/kg/min). Simultaneously, 10% glucose was infused using another infusion pump at a rate adjusted to maintain the blood glucose level at 100–140 mg/dl. Blood glucose concentration was determined every 10 min by a glucometer (LifeScan, NJ). At the end of a 120-min period, blood samples were collected (80, 90 100 and 120 min) to measure the hepatic glucose production and peripheral glucose disposal rates.

Hyperinsulinemic-euglycemic, hyperglycemic and hypoglycemic clamps of old mice (20-22 months) were carried out as described by Vanderbilt University MMPC (Berglund *et al.* 2008). Briefly, the carotid artery and jugular vein were catheterized. The arterial catheter was used for blood sampling, and the venous catheter was used for infusion in all protocols.

Mice were unrestrained and not handled thereafter to minimize stress. The experimental period (t = 0–120 min) began at >1300 h with the infusion of insulin (Humulin R; Eli Lilly) in euglycemic and hypoglycemic clamps, and glucose in hyperglycemic clamps. The steady-state period was defined as stable glycemia between t = 80–120 min. **Euglycemic clamp:** A primed continuous [3-^{3}H]glucose infusion (5-μCi bolus and 0.05 μCi/min) was given at t = −120 min to measure glucose turnover. The clamp was started at t = 0 min with a continuous insulin infusion (24 pmol/kg/min), and the [3-^{3}H] glucose was increased to 0.1 μCi/min to minimize changes in specific activity. Glucose (5 μl) was measured every 10 min, and euglycemia of ~150mg/dl was maintained using a variable glucose infusion rate. To determine glucose-specific activity, blood samples (10 μl) were taken at t = −15 and −5 min and every 10 min from t = 80-120 min. Blood samples (50 μl) were taken to measure plasma insulin at t = 0, 100, and 120 min. **Hyperglycemic clamp:** At t = 0 min, a variable glucose infusion rate was used to increase and maintain blood glucose at ~250 mg/dl. Blood glucose (5 μl) was measured at t = −15, −5, 0, 5, 10, 15, and 20 min and then every 10 min until t = 120 min. Blood samples (50 μl) were taken at various time points to measure plasma insulin and C-peptide. **Hypoglycemic clamp:** At t = 0 min, a constant insulin infusion (120 pmol/kg/min) was started to induce hypoglycemia, and a variable GIR was used to maintain blood glucose at 40-50mg/dl. Blood glucose was measured at t = −15, −5, 0, 5, 10, 15, and 20 min and then every 10 min until t = 120 min.

Determination of cell size and cell numbers of adipocytes

The H&E-stained slides of adipose tissue were analyzed with Scion Image software (Scion Corporation). Area and diameter of adipocytes were traced manually; 100 or more cells per mouse in each group were analyzed and recorded. The mean cell area was considered as equal to the mean adipocyte cell size. Mean adipocyte cell volume = π × (mean diameter)^3/6. To determine cell number, an entire lobe of epididymal fat was homogenized. Total triglyceride was extracted with chloroform:methanol (1:1) at room temperature. After centrifuging the tubes at 1000g for 10min, the clear chloroform phase was transferred to a pre-weighed tube and dried in a 60°C heat block overnight. Then, net weight was considered as total triglyceride content of the epididymal fat lobe. Number of adipocytes per lobe of epididymal fat was calculated as = total triglyceride content (g)/mean adipocyte volume (mm^3)/density (0.915) (Okuno *et al.* 1998; Pichon *et al.* 2006).

Real-time RT-PCR

Total RNA of cells was isolated using TRIzol Reagent (Invitrogen), following the manufacturer's instructions. RNA was treated with DNAse and run on the gels to validate the purity and quality of the RNA. The cDNA was synthesized from 1 μg RNA using the SuperScript III First-Strand Synthesis System for RT-PCR (Invitrogen Corp.). Real-time RT-PCR was performed on an ABI 7900 using the SYBR Green PCR Master Mix or the Taqman gene expression Master Mix (Applied Biosystems). After amplification, the PCR product was subjected to 2% agarose gel electrophoresis. 18s RNA, β-actin and 36B4 were used as internal controls. All primer and probe information are available upon request.

Western blot analyses

Tissues were lysed in RIPA buffer with Complete Protease Inhibitor Cocktail (Roche Inc.). Protein concentration was determined with BCA protein assay kit (Pierce, Rockford, IL). Twenty microgram protein of each sample was separated by SDS-PAGE, and electro-transferred to nitrocellulose membrane for immunoblot analyses. The following antibodies were used: anti-UCP1 (Millipore, 1:1000), anti-β-actin (Santa Cruz Biotechnology, 1:1000), HRP-conjugated anti-mouse (GE Healthcare UK Limited, 1:10,000), and anti-rabbit (GE Healthcare UK Limited, 1:10,000). The SuperSignal West Pico Chemiluminescent kit (Pierce) was used as substrates.

Cell culture

HIB1B pre-adipocytes were cultured in Dulbecco's modified Eagle's medium (DMEM) containing 10% bovine calf serum. At confluence (day 0), HIB1B cells were incubated in the differentiation medium {DMEM with 10% cosmic calf serum (Hyclone), supplemented with 5 μg/ml insulin (Sigma), 0.5 mM isobutylmethylxanthine (Sigma), 1 μM dexamethasone (Sigma), and 1 nM triiodothyronine (Sigma)} for 2 days. Then cells were re-fed with maintenance medium (DMEM with 10% cosmic calf serum, containing 5 μg/ml insulin and 1 nM triiodothyronine) at day 2, day 4 and day 6. Saline, 0.01nM, 1nM ghrelin (Pi Proteomics), 1μM [D-Lys^3]-GHRP-6 (Sigma) or 1nM ghrelin and 1μM [D-Lys^3]-GHRP-6 were added into the differentiation or maintenance medium at day 0, day 2, day 4 and day 6. On the 7th day of differentiation, cells were stimulated with 1 μM isoproterenol (Sigma) for 6h prior to harvest.

Statistics

Data are represented as mean ± SEM, and analyzed using statistical software SPSS by repeated measures to ANOVAs (one-way repeated measures and 2-way within-subjects to ANOVA). Statistical significance is set to a minimum of $p < 0.05$. *, $p < 0.05$, **, $p < 0.01$, ***, $p < 0.001$.

Supplementary Material

Refer to Web version on PubMed Central for supplementary material.

Acknowledgments

We gratefully acknowledge Dr. Nancy F. Butte and Mr. Firoz A. Vohra of Children's Nutrition Research Center (CNRC) for their input in the indirect calorimetry study. We thank Dr. Corey L. Reynolds and Mr. Lingyun Hu for their assistance in MRI imaging of the mice. We also thank Dr. Miao-Hsueh Chen of CNRC for her insightful critique of the manuscript, and Mr. Michael R. Honig for his excellent editorial assistance. This study was supported by NIH/NIA grant 1R03AG029641-01 (YS), USDA/CRIS grant ARS 6250-51000-055 (YS), and partly supported by the NIH-Diabetes and Endocrinology Research Center (P30DK079638) at Baylor College of Medicine. Other grants that supported the core facilities used in this study are: Vanderbilt Mouse Metabolic Phenotyping Center (U24 DK59637), Baylor Mouse Phenotyping Core (HRSA 1C76HF02799-01-00).

Abbreviations

T2D	type 2 diabetes
WAT	white adipose tissue
BAT	brown adipose tissue
UCP	uncoupling protein
GHS-R	Growth Hormone Secretagogue Receptor
IGF-1	insulin-like growth factor 1
WT	wild-type
Null	homozygous knockout
MRI	magnetic resonance imaging
FFA	free fatty acid
LDL	low density lipoproteins
VLDL	very-low density lipoproteins

HDL	high density lipoproteins
ITT	insulin tolerance tests
GTT	glucose tolerance tests
RMR	resting metabolic rate
RQ	respiratory quotient
RCF	relative cumulative frequency
PPAR	peroxisome proliferator-activated receptor
C/EBP	CCAAT-enhancer-binding protein
GLUT4	glucose transporter 4
LPL	lipoprotein lipase
aP2	adipocyte protein 2
FAS	fatty acid synthase
HSL	hormone-sensitive lipase
PEPCK	phosphoenolpyruvate carboxykinase
ABCG1	ATP-binding cassette transporter G1

References

Ahima RS. Connecting obesity, aging and diabetes. Nat Med. 2009; 15:996–997. [PubMed: 19734871]

Amati F, Dube JJ, Coen PM, Stefanovic-Racic M, Toledo FG, Goodpaster BH. Physical inactivity and obesity underlie the insulin resistance of aging. Diabetes Care. 2009; 32:1547–1549. [PubMed: 19401446]

Andrews ZB, Liu ZW, Walllingford N, Erion DM, Borok E, Friedman JM, Tschop MH, Shanabrough M, Cline G, Shulman GI, Coppola A, Gao XB, Horvath TL, Diano S. UCP2 mediates ghrelin's action on NPY/AgRP neurons by lowering free radicals. Nature. 2008; 454:846–851. [PubMed: 18668043]

Barzilai N, Banerjee S, Hawkins M, Chen W, Rossetti L. Caloric restriction reverses hepatic insulin resistance in aging rats by decreasing visceral fat. J Clin Invest. 1998; 101:1353–1361. [PubMed: 9525977]

Barzilai N, Gabriely I. The role of fat depletion in the biological benefits of caloric restriction. J Nutr. 2001; 131:903S–906S. [PubMed: 11238783]

Berglund ED, Li CY, Poffenberger G, Ayala JE, Fueger PT, Willis SE, Jewell MM, Powers AC, Wasserman DH. Glucose metabolism in vivo in four commonly used inbred mouse strains. Diabetes. 2008; 57:1790–1799. [PubMed: 18398139]

Butler AA, Kozak LP. A recurring problem with the analysis of energy expenditure in genetic models expressing lean and obese phenotypes. Diabetes. 2010; 59:323–329. [PubMed: 20103710]

Cannon B, Nedergaard J. Brown adipose tissue: function and physiological significance. Physiol Rev. 2004; 84:277–359. [PubMed: 14715917]

Cannon B, Nedergaard J. Thyroid hormones: igniting brown fat via the brain. Nat Med. 2010; 16:965–967. [PubMed: 20823876]

Choi K, Roh SG, Hong YH, Shrestha YB, Hishikawa D, Chen C, Kojima M, Kangawa K, Sasaki S. The role of ghrelin and growth hormone secretagogues receptor on rat adipogenesis. Endocrinology. 2003; 144:754–759. [PubMed: 12586750]

Cowley MA, Smith RG, Diano S, Tschop M, Pronchuk N, Grove KL, Strasburger CJ, Bidlingmaier M, Esterman M, Heiman ML, Garcia-Segura LM, Nillni EA, Mendez P, Low MJ, Sotonyi P, Friedman JM, Liu H, Pinto S, Colmers WF, Cone RD, Horvath TL. The distribution and

mechanism of action of ghrelin in the CNS demonstrates a novel hypothalamic circuit regulating energy homeostasis. Neuron. 2003; 37:649–661. [PubMed: 12597862]

Davies JS, Kotokorpi P, Eccles SR, Barnes SK, Tokarczuk PF, Allen SK, Whitworth HS, Guschina IA, Evans BA, Mode A, Zigman JM, Wells T. Ghrelin induces abdominal obesity via GHS-R-dependent lipid retention. Mol Endocrinol. 2009; 23:914–924. [PubMed: 19299444]

Feldmann HM, Golozoubova V, Cannon B, Nedergaard J. UCP1 ablation induces obesity and abolishes diet-induced thermogenesis in mice exempt from thermal stress by living at thermoneutrality. Cell Metab. 2009; 9:203–209. [PubMed: 19187776]

Festuccia WT, Blanchard PG, Turcotte V, Laplante M, Sariahmetoglu M, Brindley DN, Richard D, Deshaies Y. The PPARgamma agonist rosiglitazone enhances rat brown adipose tissue lipogenesis from glucose without altering glucose uptake. Am J Physiol Regul Integr Comp Physiol. 2009; 296:R1327–1335. [PubMed: 19211718]

Gabriely I, Ma XH, Yang XM, Atzmon G, Rajala MW, Berg AH, Scherer P, Rossetti L, Barzilai N. Removal of visceral fat prevents insulin resistance and glucose intolerance of aging: an adipokine-mediated process? Diabetes. 2002; 51:2951–2958. [PubMed: 12351432]

Gnanapavan S, Kola B, Bustin SA, Morris DG, McGee P, Fairclough P, Bhattacharya S, Carpenter R, Grossman AB, Korbonits M. The tissue distribution of the mRNA of ghrelin and subtypes of its receptor, GHS-R, in humans. J Clin Endocrinol Metab. 2002; 87:2988. [PubMed: 12050285]

Inokuma K, Ogura-Okamatsu Y, Toda C, Kimura K, Yamashita H, Saito M. Uncoupling protein 1 is necessary for norepinephrine-induced glucose utilization in brown adipose tissue. Diabetes. 2005; 54:1385–1391. [PubMed: 15855324]

Kahn SE, Hull RL, Utzschneider KM. Mechanisms linking obesity to insulin resistance and type 2 diabetes. Nature. 2006; 444:840–846. [PubMed: 17167471]

Kersten S. Mechanisms of nutritional and hormonal regulation of lipogenesis. EMBO Rep. 2001; 2:282–286. [PubMed: 11306547]

Kojima M, Kangawa K. Ghrelin: structure and function. Physiol Rev. 2005; 85:495–522. [PubMed: 15788704]

Kovsan J, Osnis A, Maissel A, Mazor L, Tarnovscki T, Hollander L, Ovadia S, Meier B, Klein J, Bashan N, Rudich A. Depot-specific adipocyte cell lines reveal differential drug-induced responses of white adipocytes--relevance for partial lipodystrophy. Am J Physiol Endocrinol Metab. 2009; 296:E315–322. [PubMed: 19033543]

Lecoultre V, Ravussin E. Brown adipose tissue and aging. Curr Opin Clin Nutr Metab Care. 2010

Longo KA, Charoenthongtrakul S, Giuliana DJ, Govek EK, McDonagh T, Qi Y, DiStefano PS, Geddes BJ. Improved insulin sensitivity and metabolic flexibility in ghrelin receptor knockout mice. Regul Pept. 2008; 150:55–61. [PubMed: 18453014]

Lopez M, Varela L, Vazquez MJ, Rodriguez-Cuenca S, Gonzalez CR, Velagapudi VR, Morgan DA, Schoenmakers E, Agassandian K, Lage R, Martinez de Morentin PB, Tovar S, Nogueiras R, Carling D, Lelliott C, Gallego R, Oresic M, Chatterjee K, Saha AK, Rahmouni K, Dieguez C, Vidal-Puig A. Hypothalamic AMPK and fatty acid metabolism mediate thyroid regulation of energy balance. Nat Med. 2010; 16:1001–1008. [PubMed: 20802499]

Mano-Otagiri A, Iwasaki-Sekino A, Nemoto T, Ohata H, Shuto Y, Nakabayashi H, Sugihara H, Oikawa S, Shibasaki T. Genetic suppression of ghrelin receptors activates brown adipocyte function and decreases fat storage in rats. Regul Pept. 2010; 160:81–90. [PubMed: 19931319]

Mattson MP. Perspective: Does brown fat protect against diseases of aging? Ageing Res Rev. 2010; 9:69–76. [PubMed: 19969105]

Miegueu P, St Pierre D, Broglio F, Cianflone K. Effect of desacyl ghrelin, obestatin and related peptides on triglyceride storage, metabolism and GHSR signaling in 3T3-L1 adipocytes. J Cell Biochem. 2011; 112:704–714. [PubMed: 21268092]

Nedergaard J, Cannon B. The changed metabolic world with human brown adipose tissue: therapeutic visions. Cell Metab. 2010; 11:268–272. [PubMed: 20374959]

Nuotio-Antar AM, Hachey DL, Hasty AH. Carbenoxolone treatment attenuates symptoms of metabolic syndrome and atherogenesis in obese, hyperlipidemic mice. Am J Physiol Endocrinol Metab. 2007; 293:E1517–1528. [PubMed: 17878220]

O'Connell J, Lynch L, Cawood TJ, Kwasnik A, Nolan N, Geoghegan J, McCormick A, O'Farrelly C, O'Shea D. The relationship of omental and subcutaneous adipocyte size to metabolic disease in severe obesity. PLoS One. 2010; 5:e9997. [PubMed: 20376319]

Okuno A, Tamemoto H, Tobe K, Ueki K, Mori Y, Iwamoto K, Umesono K, Akanuma Y, Fujiwara T, Horikoshi H, Yazaki Y, Kadowaki T. Troglitazone increases the number of small adipocytes without the change of white adipose tissue mass in obese Zucker rats. J Clin Invest. 1998; 101:1354–1361. [PubMed: 9502777]

Pfannenberg C, Werner MK, Ripkens S, Stef I, Deckert A, Schmadl M, Reimold M, Haring HU, Claussen CD, Stefan N. Impact of age on the relationships of brown adipose tissue with sex and adiposity in humans. Diabetes. 2010; 59:1789–1793. [PubMed: 20357363]

Pichon L, Huneau JF, Fromentin G, Tome D. A high-protein, high-fat, carbohydrate-free diet reduces energy intake, hepatic lipogenesis, and adiposity in rats. J Nutr. 2006; 136:1256–1260. [PubMed: 16614413]

Raz I, Eldor R, Cernea S, Shafrir E. Diabetes: insulin resistance and derangements in lipid metabolism. Cure through intervention in fat transport and storage. Diabetes Metab Res Rev. 2005; 21:3–14. [PubMed: 15386813]

Riachi M, Himms-Hagen J, Harper ME. Percent relative cumulative frequency analysis in indirect calorimetry: application to studies of transgenic mice. Can J Physiol Pharmacol. 2004; 82:1075–1083. [PubMed: 15644949]

Roberts R, Hodson L, Dennis AL, Neville MJ, Humphreys SM, Harnden KE, Micklem KJ, Frayn KN. Markers of de novo lipogenesis in adipose tissue: associations with small adipocytes and insulin sensitivity in humans. Diabetologia. 2009; 52:882–890. [PubMed: 19252892]

Roti E, Minelli R, Salvi M. Thyroid hormone metabolism in obesity. Int J Obes Relat Metab Disord. 2000; 24(Suppl 2):S113–115. [PubMed: 10997624]

Saha PK, Kojima H, Martinez-Botas J, Sunehag AL, Chan L. Metabolic adaptations in the absence of perilipin: increased beta-oxidation and decreased hepatic glucose production associated with peripheral insulin resistance but normal glucose tolerance in perilipin-null mice. J Biol Chem. 2004; 279:35150–35158. [PubMed: 15197189]

Shimbara T, Mondal MS, Kawagoe T, Toshinai K, Koda S, Yamaguchi H, Date Y, Nakazato M. Central administration of ghrelin preferentially enhances fat ingestion. Neurosci Lett. 2004; 369:75–79. [PubMed: 15380311]

Stevens, AW. The haematoxylin and eosin. Churchill Livingstone; New York: 1996. I.G.

Sun Y, Asnicar M, Saha PK, Chan L, Smith RG. Ablation of ghrelin improves the diabetic but not obese phenotype of ob/ob mice. Cell Metab. 2006; 3:379–386. [PubMed: 16679295]

Sun Y, Asnicar M, Smith RG. Central and peripheral roles of ghrelin on glucose homeostasis. Neuroendocrinology. 2007a; 86:215–228. [PubMed: 17898534]

Sun Y, Butte NF, Garcia JM, Smith RG. Characterization of adult ghrelin and ghrelin receptor knockout mice under positive and negative energy balance. Endocrinology. 2008; 149:843–850. [PubMed: 18006636]

Sun Y, Garcia JM, Smith RG. Ghrelin and growth hormone secretagogue receptor expression in mice during aging. Endocrinology. 2007b; 148:1323–1329. [PubMed: 17158206]

Sun Y, Wang P, Zheng H, Smith RG. Ghrelin stimulation of growth hormone release and appetite is mediated through the growth hormone secretagogue receptor. Proc Natl Acad Sci U S A. 2004; 101:4679–4684. [PubMed: 15070777]

Tentolouris N, Liatis S, Katsilambros N. Sympathetic system activity in obesity and metabolic syndrome. Ann N Y Acad Sci. 2006; 1083:129–152. [PubMed: 17148737]

Theander-Carrillo C, Wiedmer P, Cettour-Rose P, Nogueiras R, Perez-Tilve D, Pfluger P, Castaneda TR, Muzzin P, Schurmann A, Szanto I, Tschop MH, Rohner-Jeanrenaud F. Ghrelin action in the brain controls adipocyte metabolism. J Clin Invest. 2006; 116:1983–1993. [PubMed: 16767221]

Tschop M, Smiley DL, Heiman ML. Ghrelin induces adiposity in rodents. Nature. 2000; 407:908–913. [PubMed: 11057670]

van Marken Lichtenbelt WD, Vanhommerig JW, Smulders NM, Drossaerts JM, Kemerink GJ, Bouvy ND, Schrauwen P, Teule GJ. Cold-activated brown adipose tissue in healthy men. N Engl J Med. 2009; 360:1500–1508. [PubMed: 19357405]

Zigman JM, Nakano Y, Coppari R, Balthasar N, Marcus JN, Lee CE, Jones JE, Deysher AE, Waxman AR, White RD, Williams TD, Lachey JL, Seeley RJ, Lowell BB, Elmquist JK. Mice lacking ghrelin receptors resist the development of diet-induced obesity. J Clin Invest. 2005; 115:3564–3572. [PubMed: 16322794]

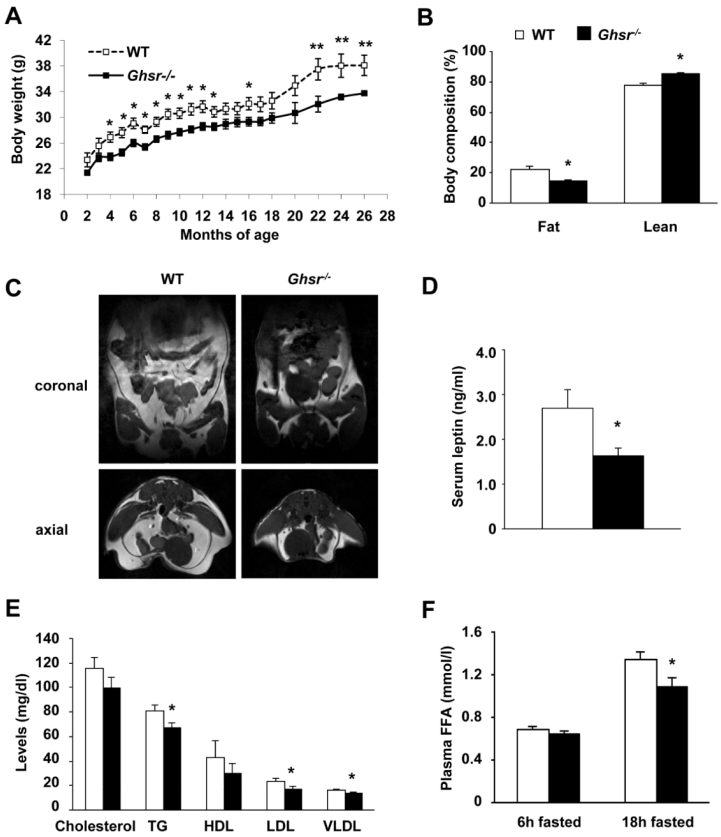

Fig. 1. GHS-R null mice display reduced adiposity and improved lipid profile

(A) Body weights of WT and *Ghsr*$^{-/-}$ mice from 2- to 26-months. n = 8-15.

(B) PIXImus scan analyses revealed that the 18-month old *Ghsr*$^{-/-}$ mice have less fat mass and more lean mass than those of WT mice (percentage of body weight). n = 8.

(C) Proton density-weighted axial MRI images of 24-month old WT and *Ghsr*$^{-/-}$ mice in both coronal and axial sections. White areas denote fat.

(D) Serum leptin level in 18-month old WT and *Ghsr*$^{-/-}$ mice after overnight fasting. n = 6.

(E) Plasma cholesterol, triglycerides, HDL, LDL, and VLDL levels in 16-month old WT and *Ghsr*$^{-/-}$ mice after 24h fasting. n = 9.

(F) Plasma free fatty acid levels of 18-month old WT and *Ghsr*$^{-/-}$ mice in the 4h and 18h fasted states. n = 9.

*, $p < 0.05$, **, $p < 0.01$, WT vs. *Ghsr*$^{-/-}$ mice.

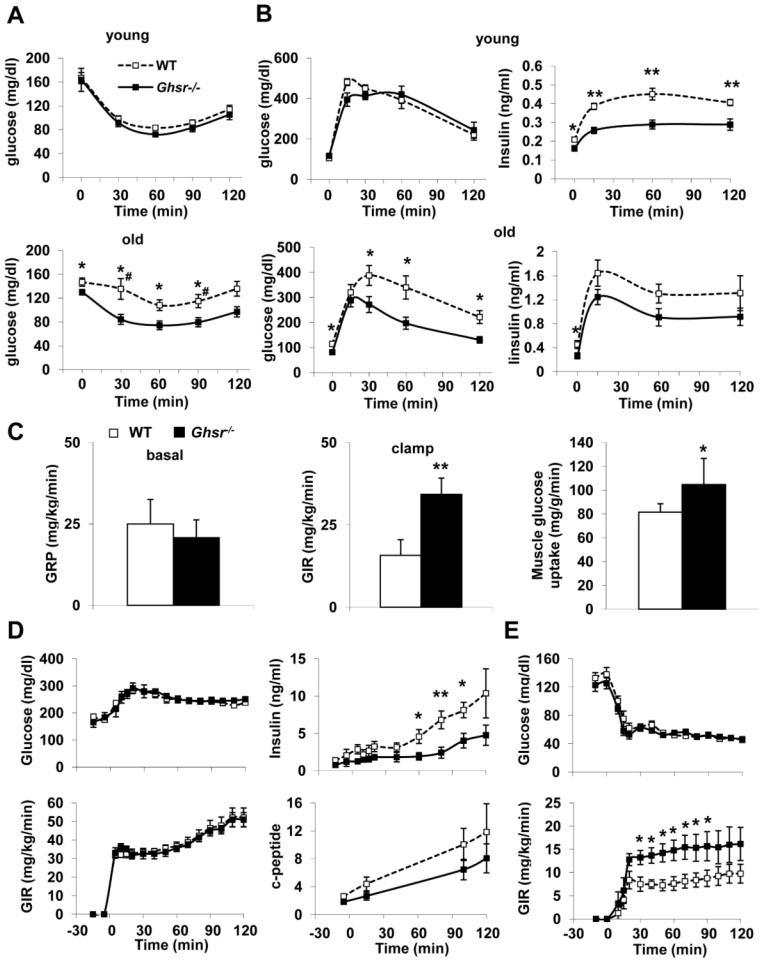

Figure 2. GHS-R null mice have improved age-associated insulin resistance

(A) Insulin tolerance tests of young (top panel, 4-month old) and old (bottom panel, 20-month old) WT and *Ghsr*$^{-/-}$ mice. $n = 9$. # indicates that when the glucose levels at 30 min and 90 min time points are calculated as percentage of baseline values (Fig. S2.A), the difference between WT and *Ghsr*$^{-/-}$ mice is still significantly different, $p < 0.05$.

(B) Glucose tolerance test of young (top panel, 4-month old) and old (bottom panel, 20-month old) WT and *Ghsr*$^{-/-}$ mice. On the left is glucose, and on the right is insulin. $n = 8$.

(C) Hyperinsulinemic-euglycemic clamp of 3-month old WT and *Ghsr*$^{-/-}$ mice. Basal glucose production is shown on the left, whole-body glucose infusion rates (GIR) during hyperinsulinemic-euglycemic clamp are shown in the middle, and muscle glucose uptake is shown on the right. $n = 6$.

(D) Hyperglycemic clamp of 18-month old WT and *Ghsr*$^{-/-}$ mice. Glucose infusion rate is shown on the left, insulin and c-peptide levels are shown on the right. $n = 10$-11.

(E) Hypoglycemic clamp of 18-month old WT and *Ghsr*$^{-/-}$ mice. Glucose infusion rate is shown on the bottom. $n = 10$.

*, $p < 0.05$, **, $p < 0.01$, WT vs. *Ghsr*$^{-/-}$ mice.

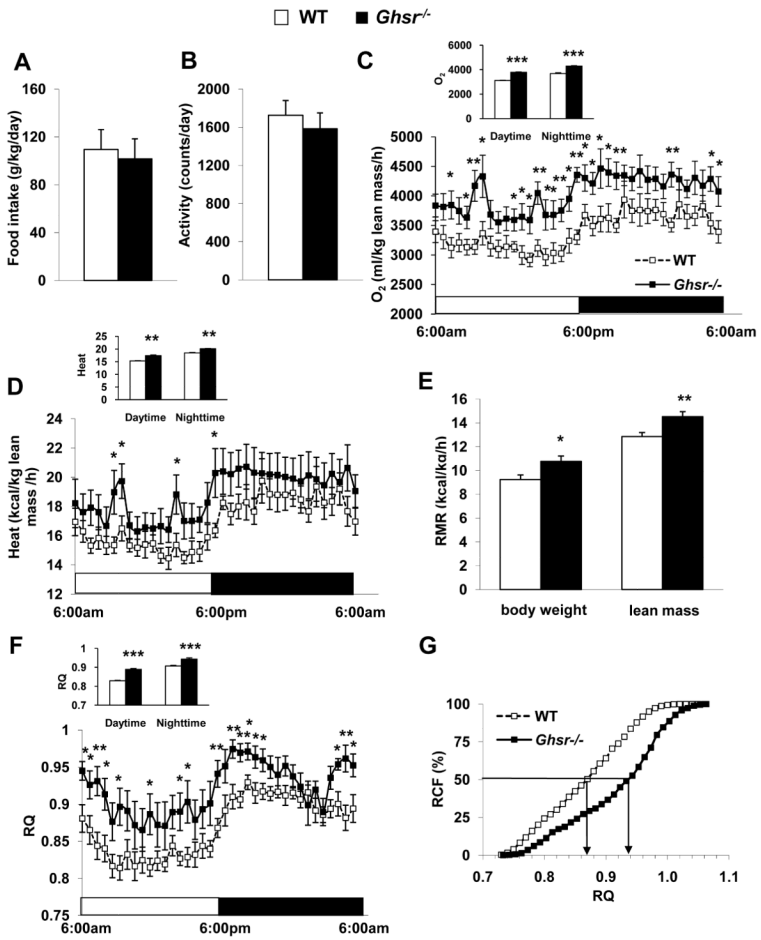

Figure 3. GHS-R null mice have increased energy expenditure and improved metabolic flexibility

22-month old WT and *Ghsr*$^{-/-}$ mice were used.

(A) Daily food intake during calorimetry.

(B) Total locomotor activity during calorimetry.

(C) Oxygen consumption (VO_2), normalized with lean mass and average values of oxygen consumption during light and dark cycles (inserts).

(D) Energy expenditure normalized with lean mass.

(E) Resting metabolic rate (RMR) was measured during light cycle, and normalized with both body weight and lean mass, respectively.

(F) Respiratory quotient (RQ) and average of RQ (inserts) during light and dark cycles.

(G) Relative cumulative frequency (RCF).

$n = 8$ for all experiments A through G. *, $p < 0.05$, **, $p < 0.01$ ***, $p < 0.001$, WT vs. *Ghsr*$^{-/-}$ mice.

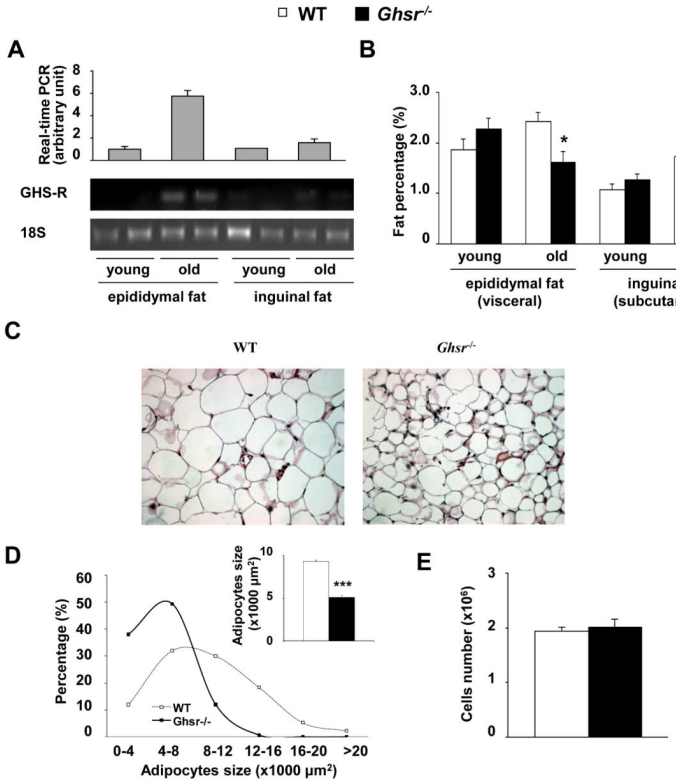

Figure 4. GHS-R null mice have reduced adipocyte cell size

4-month young and 22-month old WT and *Ghsr*$^{-/-}$ mice were used.

(A) GHS-R expression levels in WAT (epididymal and inguinal fat) were evaluated using real-time RT-PCR (top) and semi-quantitative RT-PCR (bottom).

(B) White adipose tissue (epididymal and inguinal fat) weight. $n = 8$, *, $p < 0.05$, **, $p < 0.01$ to compare WT vs. *Ghsr*$^{-/-}$ mice. #, $p < 0.05$ to compare young vs old WT.

(C) Epididymal adipocyte morphology (Representative H&E sections).

(D) The distribution of adipocyte cell size. Insert: average size of the adipocytes of WT and *Ghsr*$^{-/-}$ mice. $n = 7$, ***, $p < 0.001$, WT vs. *Ghsr*$^{-/-}$ mice.

(E) Cell numbers of whole-piece epididymal fat from WT and *Ghsr*$^{-/-}$ mice were determined by lipid content. $n = 4$.

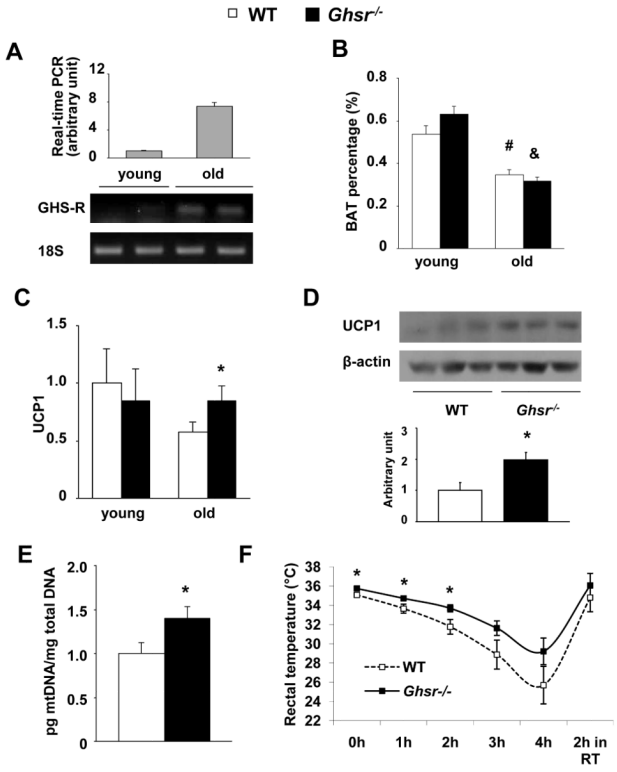

Figure 5. GHS-R is expressed in BAT of old mice and GHS-R ablation prevents against age-associated decline of thermogenic function

4-month young and 22-month old WT and *Ghsr*$^{-/-}$ mice were used.

(A) GHS-R expression levels in BAT of young and old WT were evaluated using real time RT-PCR (top) semi-quantitative RT-PCR (bottom).

(B) Brown adipose tissue weight, of young and old WT and *Ghsr*$^{-/-}$mice. $n = 8$, #, $p < 0.01$ between young vs. old WT mice; &, $p < 0.01$ between young vs. old *Ghsr*$^{-/-}$ mice.

(C) UCP1 mRNA levels in BAT of young and old WT and *Ghsr*$^{-/-}$ mice. $n = 9$.

(D) UCP1 protein levels in BAT of 22-month old WT and *Ghsr*$^{-/-}$ mice. Top panel is the representative Western blots and bottom panel is the quantization of the Westerns.

(E) Mitochondrial density was evaluated by the ratio of mitochondrial DNA(pg)/total nuclear DNA(mg) in BAT of 22-month old WT and *Ghsr*$^{-/-}$ mice. $n = 6$.

(F) Rectal temperature of 18- to 20-month old WT and *Ghsr*$^{-/-}$ mice: mice were fasted overnight in normal housing facility, then moved to 4°C cold room for 4 hours. The temperature was sampled every hour, and after 2 hour recovery in room temperature. $n = 12$. *, $p < 0.05$., WT vs. *Ghsr*$^{-/-}$ mice.

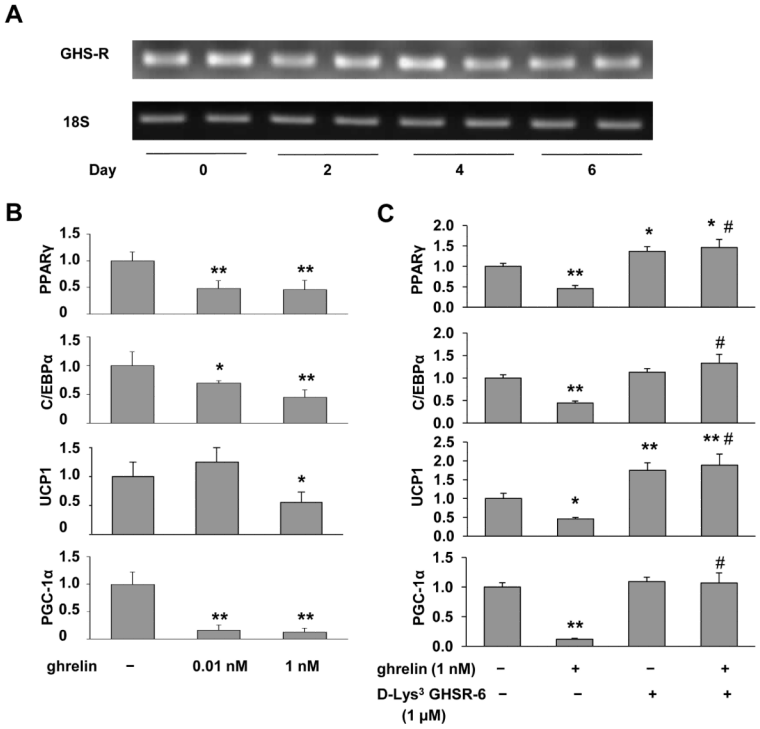

Figure 6. Ghrelin regulates brown adipocyte differentiation and UCP1 expression in HIB1B cells through GHS-R

(A) GHS-R expression in HIB1B cells during differentiation was detected with semi-quantitative RT-PCR.

(B) Real-time RT-PCR analyses of PPARγ, C/EBPα, UCP1 and PGC-1α expression in differentiated HIB1B cells treated with saline or ghrelin *, $p < 0.05$, **, $p < 0.01$, Treatments vs. Controls.

(C) Real-time RT-PCR analysis of PPARγ, C/EBPα, UCP1 and PGC-1α mRNA levels in differentiated HIB1B cells treated with saline, 1 nM ghrelin, 1 μM [D-Lys^3]-GHRP-6 or combination of ghrelin and [D-Lys^3]-GHRP-6. *, $p < 0.05$, **, $p < 0.01$, Treatments vs. Controls.

#, $p < 0.01$, Ghrelin and [D-Lys^3]-GHRP-6 combination treatment vs. Ghrelin treatment. $n = 9$, and each assay was measured in triplicate.

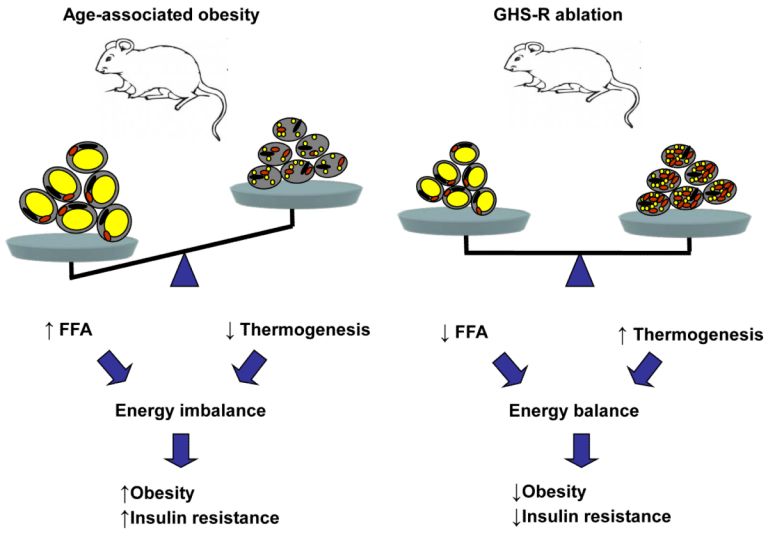

Figure 7. The schematic diagram of the role of GHS-R ablation in fat metabolism during aging

Data summary and interpretation: Aging is associated with increased adiposity and impaired thermogenesis, which results in energy imbalance and subsequently leads to obesity and insulin resistance (left panel). GHS-R ablation reduces adiposity in white adipose tissues and increases thermogenesis in brown adipose tissues. This allows the animals to maintain an energy balanced state, subsequently leading to reduced obesity and improved insulin sensitivity (right panel).

Table 1

The mRNA Expression of Adipogenic, Lipogenic, Lipolytic, and Lipid Recycling Genes in Epididymal Adipose Tissue

Transcripts	WT	*Ghsr*−/−	*P* Value
Adipogenic			
PPARγ2	1.00 ± 0.12	0.76 ± 0.09	**<0.05**
C/EBPα	1.00 ± 0.09	1.23 ± 0.20	0.26
Glucose/Lipid Uptake			
GLUT4	1.00 ± 0.12	0.54 ± 0.10	**<0.001**
Lipoprotein lipase	1.00 ± 0.09	0.58 ± 0.11	**<0.001**
CD36	1.00 ± 0.14	0.54 ± 0.11	**<0.001**
Lipogenic			
aP2	1.00 ± 0.12	0.61 ± 0.11	**<0.001**
Fatty acid synthase	1.00 ± 0.09	0.50 ± 0.09	**<0.001**
Lipin 1	1.00 ± 0.09	0.58 ± 0.10	**<0.001**
Lipid Utilization			
UCP2	1.00 ± 0.11	0.90 ± 0.10	0.26
Lipolytic			
Perilipin	1.00 ± 0.13	0.69 ± 0.11	**<0.05**
HSL	1.00 ± 0.09	0.83 ± 0.11	**<0.05**
Lipid Recycling			
PEPCK	1.00 ± 0.08	0.56 ± 0.07	**<0.001**
Cholesterol Exporter			
ABCG1	1.00 ± 0.12	0.82 ± 0.13	0.07

Values shown are mean ± SEM (n = 9 -16). The age of the mice range from 20-months to 24-months.

Table 2

The mRNA Expression of Thermogenic and Lipid Metabolic genes in Brown Adipose Tissue (BAT)

Transcripts	WT	*Ghsr*−/−	*P* Value
Lipid metabolic genes			
Adipogenic			
PPARγ2	1.00 ± 0.12	1.27 ± 0.14	0.07
C/EBPα	1.00 ± 0.14	1.38 ± 0.16	**<0.01**
Glucose/Lipid Uptake			
GLUT4	1.00 ± 0.09	1.39 ± 0.11	**<0.001**
Lipoprotein lipase	1.00 ± 0.08	1.80 ± 0.15	**<0.001**
CD36	1.00 ± 0.07	1.15 ± 0.10	**<0.05**
Lipogenic			
aP2	1.00 ± 0.08	1.52 ± 0.12	**<0.001**
Fatty acid synthase	1.00 ± 0.14	1.07 ± 0.16	0.65
Lipin1	1.00 ± 0.14	1.34 ± 0.17	**<0.05**
Lipid Utilization			
UCP2	1.00 ± 0.12	1.06 ± 0.12	0.48
Lipolytic			
Perilipin	1.00 ± 0.13	1.90 ± 0.28	**<0.05**
HSL	1.00 ± 0.18	1.13 ± 0.15	0.40
Lipid Recycling			
PEPCK	1.00 ± 0.12	1.32 ± 0.16	0.06
Thermogenic genes			
UCP1	1.00 ± 0.11	1.70 ± 0.22	**<0.01**
PGC-1α	1.00 ± 0.19	1.81 ± 0.30	0.08

Values shown are mean ± SEM (n = 9 -12). The age of the mice range from 20-months to 24-months.